

# SAM Decoding: Speculative Decoding via Suffix Automaton

**Yuxuan Hu<sup>1,2</sup>, Ke Wang<sup>1,2</sup>, Xiaokang Zhang<sup>1,2</sup>, Fanjin Zhang<sup>4</sup>  
Cuiping Li<sup>1,3</sup>, Hong Chen<sup>1,3</sup>, Jing Zhang<sup>1,3\*</sup>**

<sup>1</sup>School of Information, Renmin University of China, Beijing, China

<sup>2</sup>Key Laboratory of Data Engineering and Knowledge Engineering, Beijing, China

<sup>3</sup>Engineering Research Center of Database and Business Intelligence, Beijing, China

<sup>4</sup>Knowledge Engineering Group, Tsinghua University, Beijing, China

## Abstract

Large Language Models (LLMs) have revolutionized natural language processing by unifying tasks into text generation, yet their large parameter sizes and autoregressive nature limit inference speed. SAM-Decoding addresses this by introducing a novel retrieval-based speculative decoding method that uses a suffix automaton for efficient and accurate draft generation. Unlike n-gram matching used by the existing method, SAM-Decoding finds the exact longest suffix match in generating text and text corpus, achieving an average time complexity of  $O(1)$  per generation step. Meanwhile, based on the exact match length, it is designed as an approach that can be combined with existing methods, allowing SAM-Decoding to adaptively select a draft generation strategy based on the matching length, thus increasing the inference speed of the LLM. When combined with Token Recycling, evaluations show SAM-Decoding outperforms existing model-free methods, achieving a speedup of  $2.27\times$  over autoregressive decoding on Spec-Bench. When combined with EAGLE2, it reaches a speedup of  $2.49\times$ , surpassing all current approaches. Our code is available at [ours repository](#).

## 1 Introduction

The Transformer-based Large Language Model (Brown et al., 2020; Dubey et al., 2024; Yang et al., 2024) has become a foundation model in the field of natural language processing. Through the large language model (LLM), all natural language processing tasks are unified as text generation tasks, which greatly improves the convenience of solving natural language processing tasks. While LLM has shown good performance in various tasks and is easy to use, the large-scale parameters and text generation-based paradigm contained in LLM have brought challenges to

the practical deployment, especially in terms of the inference speed of the LLM. LLM generates tokens step by step in an autoregressive manner. At each round of generation, LLM generates one new token based on the tokens that has been generated. In addition, for the GPUs used for deploy LLM, this process requires reading the huge number of parameters contained in the LLM from the High-Bandwise Memory (HBM) to the on-chip memory, but these parameters only operate on a small number of parameters corresponding to the new token, resulting in the inability to fully utilize the parallel capabilities of the modern GPU, thereby limiting the inference speed of the LLM.

To address the above problem, one effective strategy is to enhance the arithmetic intensity of the large language model (LLM) generation process, which involves reducing the number of generation rounds while increasing the number of tokens generated in each round. Building upon this concept, the method of speculative decoding has been introduced and has spurred a series of follow-up studies (Leviathan et al., 2023; Miao et al., 2024; Cai et al., 2024; Fu et al., 2024). Rather than generating a single token per step, these approaches employ a draft model to predict token sequence as draft. The predicted sequence are then verified against the LLM, and only the accurate tokens are adopted.

Most speculative decoding techniques employ various neural networks, such as smaller language models (LLMs) or embedding layers, as draft models, which we categorize as model-based methods. Although model-based speculative methods perform well on all kinds of tasks, when we consider some special tasks such as summarization, rewriting, there is a simpler type of speculative decoding methods that exhibit superior performance, which we call retrieval-based speculative decoding methods. These methods involve retrieving potential subsequent tokens from previously generated content or a text database during each generation round.

\*Corresponding author.

Unlike model-based approaches, retrieval-based methods do not necessitate the training of draft models or the use of GPUs for inference.

After examining the current retrieval-based methods, we identify several limitations. Firstly, these approaches typically rely on a single retrieval source. For instance, PLD (Saxena, 2023) focuses solely on prompts, whereas REST (He et al., 2024) is limited to text corpus. Secondly, there are limitations in the retrieval techniques they adopt; PLD relies on n-gram matching, which is fast for context matching but cannot be extended to a wider range of textual repositories due to its poor theoretical complexity, while REST is based on suffix arrays, which has better complexity but cannot be applied to continually generating text. Lastly, not every step in the generation is suitable for the retrieval method; in a few generation steps, a large number of tokens can be accepted based on PLD and REST, but in the rest of the generation steps there is no acceleration.

To address the limitations of the retrieval-based approach mentioned earlier, this paper introduces SAM-Decoding, an innovative retrieval-based speculative decoding technique. Unlike existing approaches that rely on n-gram matching, SAM-Decoding employs a suffix automaton (SAM) to solve the exact longest suffix match problem for the generating text within both the historical generated text and the text corpus. This process yields more accurate match positions and exact match lengths compared to n-gram matching. Moreover, during the text generation phase, the suffix automaton effectively captures the relationships between adjacent suffixes, ensuring that the average time complexity for identifying the longest suffix match at each step remains at  $O(1)$ . This represents a significant improvement over the theoretical computational efficiency of n-gram matching. Meanwhile, the length of the longest suffix match serves as an indicator of the alignment between the generating text and retrieval sources. By exploiting this metric, our approach can integrate existing speculative decoding methods as an auxiliary and dynamically decide whether to generate a draft based on the matched content, or utilize an auxiliary decoding method. This adaptability leads to a notable increase in the overall speed of the text generation process.

Specifically, SAM-Decoding first constructs a static suffix automaton for the existing text corpus. For each request, SAM-Decoding then builds a dy-

namic suffix automaton based on the input prompt. The suffix automaton contains a series of nodes, each of which corresponds to several substrings in the context (text corpus, prompt and generating text). We record the earliest corresponding position of each node in the text. This information facilitates the generation of drafts by directly mapping nodes in the automaton to indices in the context. We also maintain the corresponding nodes of the generating text in both the static and dynamic automaton. Therefore, in each round of generation, we can directly retrieve the draft from the context according to the position recorded in the node, and filter the draft according to the matching length. After generation, as new tokens are generated, for the static automaton, we transition nodes of SAM based on new tokens, and for the dynamic automaton, we first expand the structure to accommodate the new tokens before transitioning nodes of SAM accordingly.

Extensive evaluations across a range of tasks indicate that the SAM-Decoding can achieve results that are competitive with existing state-of-the-art (SOTA) approaches in all tasks. Particularly in tasks where retrieval-based methods are applicable, SAM-Decoding outperforms all existing methods. On Spec-Bench, the latest benchmark for speculative decoding, SAM-Decoding combined with Token Recycling (Luo et al., 2024) achieves a speedup of 2.26 times compared to autoregressive decoding, outperforming all model-free baselines. Additionally, when SAM-Decoding is combined with EAGLE2 (Li et al., 2024a), the SOTA model-based speculative decoding method, it achieves a speedup of 2.49 times compared to autoregressive decoding, outperforming all existing model-based and model-free methods.

## 2 Background

### 2.1 Suffix Automaton

Suffix Automaton is an efficient data structure for representing the substring index of a given string, which allows fast substring retrieval. The time complexity of constructing a suffix automaton is  $O(L)$ , where  $L$  is the length of the string and it can be constructed incrementally.

A suffix automaton contains a series of nodes and two types of state transfer edges, **extension edges** and **suffix link edges**. A node in the automaton represents a state and corresponds to all substrings that have the same ending position in

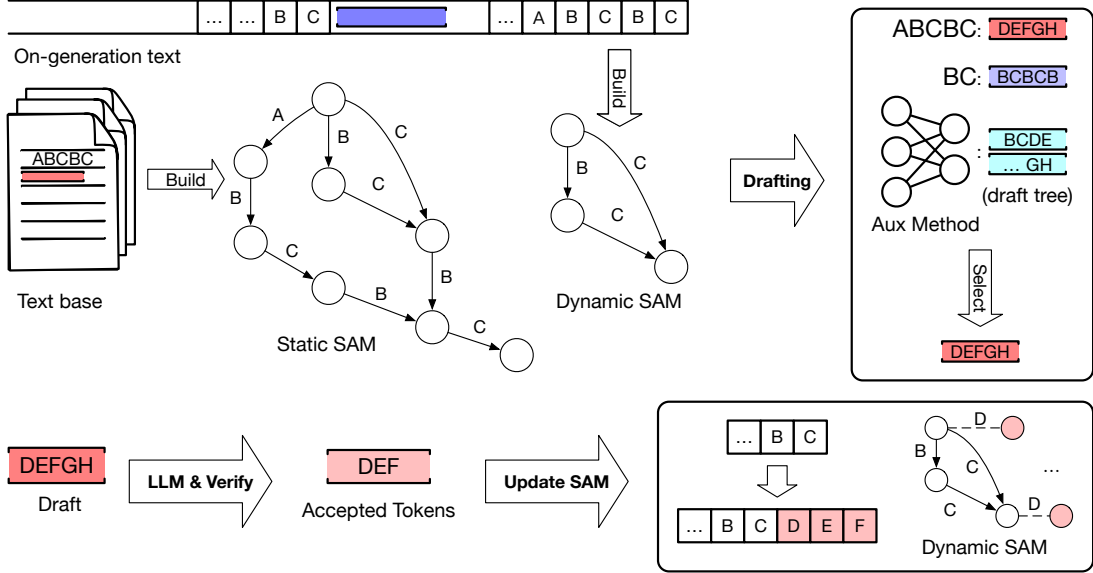


Figure 1: Overview of SAM-Decoding’s workflow. SAM-Decoding includes two automaton: static SAM and dynamic SAM. Among them, the static SAM is built based on a given text corpus, while the dynamic SAM is built based on generating text and gradually expanded during the generation process. When drafting, the suffix automaton matches the suffixes of the generating text and retrieves the draft from the text corpus and the generating text respectively according to the matching position. Meanwhile, we also combined an auxiliary speculative decoding algorithm (Aux Method) to deal with scenarios where retrieval is not applicable. we select the draft to be used from the three candidate drafts based on the match length. After that, the draft will be verified by LLM to obtain accepted tokens. Using these accepted tokens, we finally extend the dynamic SAM and generating text for the next round of generation.

the string. Meanwhile, extension edges are standard edges that represent a possible extension of the current substring by appending a new character, while suffix link edges create a path that allows the automaton to quickly jump to states representing shorter suffixes of the current substring.

Based on the two types of transfer edges, for a progressively generated token sequence, we can find the longest suffix that matches the sequence in a suffix automaton at each step of the generation with an average  $O(1)$  time complexity.

## 2.2 Speculative Decoding

Given the model input  $x = (x_1, x_2, \dots, x_t)$ , an LLM generates a new token  $x_{t+1}$  at each generation step autoregressively. The key idea of speculative decoding is to utilize a lightweight draft model to generate multiple candidate tokens quickly, i.e.,  $x_{\text{draft}} = (x_{t+1}, x_{t+2}, \dots, x_{t+n})$ , and then the target LLM simultaneously evaluates these candidates and accept those aligned with the output distribution of the LLM, i.e.,  $x_{\text{accept}} = (x_{t+1}, x_{t+2}, \dots, x_{t+m})$ .

In the above, we assume that the draft is a sequence of tokens. Recent works proposed to generate a candidate token tree via a tree mask in the

attention module to make the target LLM simultaneously evaluate multiple branches of this token tree, thereby increasing the acceptance length of the draft model.

## 3 SAM-Decoding

In this section, we introduce our proposed method, SAM-Decoding. SAM-Decoding is a retrieval-based speculative decoding method designed to address three key limitations in existing retrieval-based speculative methods: **(1)** The use of insufficient retrieval sources. **(2)** The employment of inefficient retrieval methods and restrictions on  $n$ -gram matching lengths. **(3)** Subpar performance outside specialized domains (e.g., summarization and RAG tasks).

To tackle the first two limitations, SAM-Decoding leverages suffix automaton, which significantly enhances the coverage of retrieved corpus and the efficiency of the retrieval process while allowing for more flexible matching lengths. In what follows, we detail how SAM-Decoding can be integrated with both model-free and model-based methods. By utilizing the precise matching information provided by the suffix automaton, our method not

only overcomes the third limitation but also ensures consistent performance improvements across a wide range of tasks.

### 3.1 Suffix Automaton Construction

SAM-Decoding facilitates rapid draft generation by leveraging suffix automaton. Unlike traditional methods that rely on a single retrieval source, our approach utilizes both a text corpus and the generating text itself as retrieval sources. To accommodate these dual sources, we construct two distinct types of suffix automaton: a static suffix automaton and a dynamic suffix automaton. For the text corpus, we pre-build a static suffix automaton offline. During the inference phase, state matching is performed exclusively on this static automaton. Conversely, for the generating text, we create a dynamic suffix automaton that incrementally expands as the text generation progresses. State matching is also carried out concurrently with this expansion.

A suffix automaton can be constructed in linear time using Blumer’s algorithm (Blumer et al., 1984). Since the suffix automaton is designed for a single reference string, when dealing with multiple strings in the text corpus, we concatenate them into a single long string using special symbols, such as an End-of-Sentence (EOS) token. We then construct a static suffix automaton for this concatenated string.

At the same time, we also made several modifications to the suffix automaton to better suit draft generation. Specifically, at each generation step, the generating text corresponds to a node in the automaton, representing the longest suffix match. We need to identify the matching position in either the text corpus or the generating text. Based on this position, we can use the subsequent tokens as potential drafts. To achieve this, at every node of the suffix automaton, we record the earliest position of all substrings corresponding to that node in the reference string. We define this position as **min\_endpos**. By using the **min\_endpos**, we can directly map node to the position in the reference string. The construction process of the suffix automaton is detailed in Appendix A.1.

### 3.2 Drafting with Suffix Automaton

After constructing the suffix automaton, it can be utilized as a draft model to generate draft at each step of the generation process. Specifically, let the current input to the LLM be denoted as  $x = (x_1, x_2, \dots, x_t)$ , with the predicted next to-

ken being  $x_{t+1}$ . We define the suffix automaton as  $S$  and its associated reference text as  $T$ . The state within the suffix automaton corresponding to the sequence  $x$  is denoted as  $s_t$ . The transition to the next state is performed based on the newly generated token  $x_{t+1}$  and the current state  $s_t$ :

$$s_{t+1} = \text{Transfer}(S, x_{t+1}, s_t).$$

Subsequently, we extract  $n$  consecutive tokens from the reference text  $T$  to form a draft, using the **min\_endpos** value stored in node corresponding to state  $s_{t+1}$ . If the **min\_endpos** value in  $s_{t+1}$  is  $p_{t+1}$ , then the draft  $d$  is defined as:

$$d = T[p_{t+1} : p_{t+1} + n],$$

where  $d$  represents the generated draft and  $n$  denotes the length of the draft.

In practical use, we utilize two types of automaton: a static automaton for the text corpus and a dynamic automaton for generating text. To distinguish between the two, we explicitly record the attribute  $l_{t+1}$  for the state  $s_{t+1}$ . This attribute represents the longest suffix length matched by the generating text in the automaton. This helps us determine whether the draft should be generated using the static suffix automaton or the dynamic suffix automaton. Our experimental findings indicate that drafts generated from the dynamic automaton often outperform those from the static text corpus. Consequently, we prioritize drafts from the dynamic automaton. Specifically, let  $l_1$  and  $l_2$  represent the matching lengths of the static automaton and the dynamic automaton, respectively. We use the draft provided by the static automaton only if  $l_1 > l_2 + l_{\text{bias}}$ ; otherwise, we use the draft provided by the dynamic automaton. Here,  $l_{\text{bias}}$  is a predefined constant greater than 0.

We illustrate the state transfer process of the suffix automaton in Algorithm 1. Using amortized analysis, we can prove that the average complexity of state transfer is  $O(1)$ , while the worst-case time complexity is  $O(L)$ , where  $L$  represents the length of the generating text. The detailed proof is provided in Appendix A.2. Reviewing existing methods, PLD uses  $n$ -grams and performs a brute-force search for matches in the prompt, resulting in a time complexity of  $O(n^2 L)$ . REST also employs  $n$ -grams but searches for matches in the text using suffix arrays, leading to a time complexity of  $O(n^2 \log L)$ . Here,  $n$  represents the predefined maximum matching length, and  $L$  represents the

---

**Algorithm 1** State Transfer of Suffix Automaton

---

```
function Transfer
    Input: suffix automaton  $S$ , next token  $t$ , current state  $s$ , current matching length  $l$ 
    while  $s \neq S.\text{root}$  and  $t \notin s.\text{next}$  do
         $s = s.\text{link}$ 
         $l = s.\text{length}$ 
    end while
    if  $t \in s.\text{next}$  then
         $s = s.\text{next}[t]$ 
         $l = l + 1$ 
    else
         $l = 0$ 
    end if
    return  $s, l$ 
end function
```

---

length of the prompt and the total text in the corpus, respectively. In comparison, our proposed model (SAM-Decoding) has a lower time complexity. Additionally, SAM-Decoding can find the exact longest suffix match without any limit on the matching length. This means that SAM-Decoding can generate drafts both faster and more accurately.

### 3.3 Update of Suffix Automaton

After the draft is generated, we verify the draft using the large language model (LLM) and accept the correct tokens from the draft. Let the accepted tokens be denoted as  $x_{\text{accept}} = (x_{t+1}, x_{t+2}, \dots, x_{t+m})$ . We then update the state of the suffix automaton based on these accepted tokens. For the static suffix automaton, we simply transfer the matching states according to Algorithm 1:

$$s_{t+i} = \text{Transfer}(S, s_{t+i-1}, x_{t+i}), i \in \{1, 2, \dots, m\}$$

For the dynamic suffix automaton, we first expand its state based on the accepted tokens and then transfer the matching state. Let  $S_t$  denote the dynamic suffix automaton corresponding to the generated text  $(x_1, x_2, \dots, x_t)$ . The process is as follows:

$$S_{t+i} = \text{Expand}(S_{t+i-1}, x_{t+i}), i \in \{1, 2, \dots, m\},$$
$$s_{t+i} = \text{Transfer}(S_{t+m}, s_{t+i-1}, x_{t+i}), i \in \{1, 2, \dots, m\}$$

where the process of expanding the suffix automaton is detailed in Appendix A.1.

### 3.4 Adaptive Draft Selection

A straightforward idea is that the length of the suffix match can indicate the quality of the draft produced by the automaton. A longer match suggests that more tokens from the draft are likely to be acceptable, whereas a shorter match implies that the draft contains less useful information. Consider that besides the retrieval-based speculative decoding approach, there exist various alternative speculative decoding techniques. Consequently, if the retrieval-based method fails to produce a satisfactory draft, we can resort to these alternatives to enhance the draft’s effectiveness.

To implement this, we concurrently employ an additional speculative decoding technique alongside the suffix automaton. During each iteration of the generation process, we adaptively select between the draft offered by the automaton and that provided by the supplementary speculative decoding method, based on the match length of the generated text within the automaton. The adaptive draft selection procedure is detailed in Algorithm 2, where  $l_{\text{threshold}}$  denotes a predetermined constant that determines whether to utilize the automaton or the auxiliary speculative decoding for draft generation. In our study, we incorporate two cutting-edge speculative decoding methods as auxiliary options: the model-free Token Recycling and the model-based EAGLE. Among them, Token Recycling maintains an adjacency list of the top  $k$  probable next tokens for each token. During each generation step, a draft tree is built using this adjacency list via breadth-first search, with the list being continuously updated according to the latest generated tokens. Conversely, EAGLE constructs a draft tree in each generation cycle by leveraging a Transformer decoder layer that integrates the hidden states output by the LLM.

## 4 Experiments

In this section, we first introduce our experimental setup, then present the experimental results, and finally present the ablation experiments.

**Models and tasks.** We conducted experiments on Vicuna-7B-v1.3 (Zheng et al., 2023). We evaluated SAM-Decoding on Spec-Bench (Xia et al., 2024), HumanEval (Chen et al., 2021), MBPP (Austin et al., 2021), and HARGID (Kamalloo et al., 2023). Spec-Bench is a comprehensive benchmark designed for assessing Speculative Decoding methods across diverse scenarios. It is based on six

Model	Method	Multi-turn Conversation	Translation	Summarization	Question Answering	Mathematical Reasoning	Retrieval-aug. Generation	#Mean Accepted Tokens	Tokens/s	Overall
Vicuna-7B	Lookahead	1.29 $\times$	1.03 $\times$	1.22 $\times$	1.07 $\times$	1.41 $\times$	1.13 $\times$	1.62	44.37	1.19 $\times$
	REST	1.59 $\times$	1.22 $\times$	1.27 $\times$	1.45 $\times$	1.38 $\times$	1.36 $\times$	1.63	51.34	1.38 $\times$
	PLD	1.60 $\times$	0.95 $\times$	2.44 $\times$	1.18 $\times$	1.59 $\times$	1.72 $\times$	1.75	59.02	1.56 $\times$
	<b>SAM-Decoding</b>	1.75 $\times$	0.99 $\times$	2.54 $\times$	1.24 $\times$	1.74 $\times$	1.71 $\times$	1.89	62.26	1.65 $\times$
	Token Recycling	1.92 $\times$	1.61 $\times$	1.96 $\times$	1.71 $\times$	2.16 $\times$	1.68 $\times$	2.83	69.65	1.84 $\times$
	<b>SAM-Decoding[T]</b>	2.48 $\times$	1.73 $\times$	2.86 $\times$	1.98 $\times$	2.44 $\times$	2.14 $\times$	3.03	85.73	2.27 $\times$
	EAGLE	2.63 $\times$	1.92 $\times$	2.28 $\times$	2.11 $\times$	2.64 $\times$	1.95 $\times$	3.57	85.71	2.27 $\times$
	<b>SAM-Decoding[E]</b>	2.78 $\times$	1.88 $\times$	2.65 $\times$	2.12 $\times$	2.57 $\times$	2.10 $\times$	3.77	88.99	2.35 $\times$
	EAGLE2	2.87 $\times$	1.92 $\times$	2.33 $\times$	2.20 $\times$	2.88 $\times$	2.03 $\times$	4.36	90.14	2.38 $\times$
	<b>SAM-Decoding[E2]</b>	3.02 $\times$	1.89 $\times$	2.76 $\times$	2.19 $\times$	2.83 $\times$	2.23 $\times$	4.61	94.17	2.49 $\times$

Table 1: Speedup of SAM-Decoding compared to the baselines on Spec-Bench.

Model	Method	HumanEval			MBPP			HAGRID		
		#MAT	Tokens/s	Speedup	#MAT	Tokens/s	Speedup	#MAT	Tokens/s	Speedup
Vicuna-7B	PLD	1.65	59.04	1.52 $\times$	1.42	50.62	1.27 $\times$	2.03	44.11	1.29 $\times$
	Token Recycling	2.78	75.44	1.94 $\times$	2.83	79.22	1.99 $\times$	2.88	66.17	1.93 $\times$
	<b>SAM-Decoding[T]</b>	2.94	95.08	2.45 $\times$	2.87	94.50	2.37 $\times$	3.23	87.93	2.57 $\times$
	EAGLE	4.10	103.39	2.66 $\times$	4.17	119.31	3.00 $\times$	3.44	72.14	2.11 $\times$
	<b>SAM-Decoding[E]</b>	4.03	110.16	2.83 $\times$	3.85	114.92	2.87 $\times$	4.05	93.17	2.72 $\times$
	EAGLE2	5.12	128.19	3.30 $\times$	5.29	135.24	3.40 $\times$	4.15	82.61	2.41 $\times$
	<b>SAM-Decoding[E2]</b>	4.79	127.03	3.27 $\times$	4.50	117.06	2.94 $\times$	4.75	96.60	2.81 $\times$

Table 2: Speedup of SAM-Decoding compared to the baselines on HumanEval, MBPP, and HAGRID.

commonly used datasets, MT-Bench (Zheng et al., 2023), WMT14 DE-EN, CNN/Daily Mail (Nallapati et al., 2016), Natural Question (Kwiatkowski et al., 2019), GSM8K (Cobbe et al., 2021), and DPR (Karpukhin et al., 2020), including six aspects: Multi-turn Conversation, Translation, Summarization, Question Answering, Mathematical Reasoning, and Retrieval-augmented Generation. In addition, MBPP, HumanEval, and HAGRID are used to evaluate the speed of decoding methods in code generation tasks and contextual question answering tasks, respectively.

**Baselines.** We considered the following baseline methods, including the model-based method EAGLE (Li et al., 2024b,a), the model-free methods Token Recycling (Luo et al., 2024) and Lookahead Decoding (Fu et al., 2024), and the retrieval-based methods PLD (Saxena, 2023) and REST (He et al., 2024).

**Metrics.** We evaluated speculative decoding methods from the following aspects (Li et al., 2024b)

- **Speedup Ratio:** The wall-time speedup ratio of speculative decoding methods compared to autoregressive generation methods.

- **Mean Accepted Tokens:** The average number of tokens accepted per generation step.
- **Throughput:** The average number of tokens generated per second.

**Experiment setup.** We conducted experiments on a server equipped with a 20-core CPU and a single NVIDIA RTX A6000 GPU (48GB). The experiments were implemented using PyTorch 2.3.0 and CUDA 12.1. For the models, we used the float16 data type and applied greedy decoding with a batch size of 1. Regarding hyperparameters, unless otherwise specified,  $l_{\text{bias}}$  and  $l_{\text{threshold}}$  were set to 5, and the size of the draft generated by the automaton was set to 40 tokens. For the auxiliary speculative decoding algorithms, we used the default configurations as described in their respective original papers. One exception was made for Token Recycling: instead of the draft tree structure used in the original paper, we employed a draft tree with a depth of 6 and containing 60 nodes. In addition, for the vicuna model, we use the vicuna template to convert prompt and output into the chat form, and for the Llama3 model, we use the template provided in the EAGLE2 repository.

For SAM-Decoding, we constructed a static

---

**Algorithm 2** Adaptive Draft Selection

---

```
function Drafting
    Input: static suffix automaton  $S_{\text{static}}$ , dynamic suffix automaton  $S_{\text{dyn}}$ , auxiliary speculative method  $A$ , next token  $t$ 
     $d_1, l_1 = \text{Drafting}(S_{\text{static}}, t)$ 
     $d_2, l_2 = \text{Drafting}(S_{\text{dyn}}, t)$ 
    if  $l_1 > l_2 + l_{\text{bias}}$  then
         $d = d_1$ 
         $l = l_1$ 
    else
         $d = d_2$ 
         $l = l_2$ 
    end if
    if  $l \geq l_{\text{threshold}}$  then
        return  $d$ 
    else
        return  $\text{Drafting}(A, t)$ 
    end if
end function
```

---

suffix automaton based on the Stanford-alpaca, python-code-instruction-18k, and GSK8k. To enhance our model, we incorporated two auxiliary approaches: the model-free method Token Recycling and the model-based method EAGLE. Here, SAM-Decoding[T], SAM-Decoding[E], and SAM-Decoding[E2] denote the combinations of our base model with Token Recycling, EAGLE, and EAGLE2, respectively.

**Experiment Results.** Experiment results on Spec-Bench when using Vicuna-7B-v1.3 are shown in Table 1. In the Spec-Bench, which consists of six tasks, multturn conversation, summarization, and retrieval-augmented generation were identified as particularly amenable to retrieval techniques. The results indicate that integrating SAM-Decoding into these tasks led to notable speed improvements. Specifically, for Token Recycling, the speedup ratio for the three tasks rose from  $1.92\times$ ,  $1.96\times$ , and  $1.68\times$  to  $2.48\times$ ,  $2.86\times$ , and  $2.14\times$ , respectively. With EAGLE, the speedup ratio increased from  $2.63\times$ ,  $2.28\times$ , and  $1.95\times$  to  $2.78\times$ ,  $2.65\times$ , and  $2.10\times$ , respectively. For EAGLE2, the speedup ratios went up from  $2.87\times$ ,  $2.33\times$ , and  $2.03\times$  to  $3.02\times$ ,  $2.76\times$ , and  $2.23\times$ , respectively. However, for the remaining tasks, the drafts produced by the retrieval methods did not significantly aid speculative decoding and instead introduced extra computational costs, leading

to slight decreases in performance. Despite this, when SAM-Decoding was combined with these existing methods, there was an overall increase in speedup ratios: from  $2.83\times$  to  $2.98\times$  for Token Recycling, from  $3.57\times$  to  $3.77\times$  for EAGLE, and from  $2.38\times$  to  $2.49\times$  for EAGLE2. It is noteworthy that in the summarization task, the model-free approach (SAM-Decoding[T]) outperformed the model-based method, achieving a speedup ratio of  $2.86\times$ . Meanwhile, these results also underscore the potential benefits of integrating SAM-Decoding with different auxiliary strategies, especially in tasks where retrieval can effectively support the decoding process.

Table 2 presents the experimental results on the HumanEval, MBPP, and HAGRID datasets when using Vicuna-7B-v1.3. For the coding datasets HumanEval and MBPP, we constructed static suffix automata based on the python-code-instructions-18k dataset. For the contextual question answering dataset HAGRID, we built a static suffix automaton using its own training set.

In the case of coding tasks, SAM-Decoding significantly accelerates the model-free method. When SAM-Decoding is combined with Token Recycling, the speedup ratios improve from  $2.78\times$  and  $2.83\times$  to  $2.94\times$  and  $2.87\times$  on the HumanEval and MBPP datasets, respectively. Notably, SAM-Decoding demonstrates a more pronounced acceleration effect on HumanEval. This is attributed to the fact that HumanEval often features longer, more semantically rich variable names and includes additional annotations in the input prompts. These conditions are favorable for retrieval-based methods. Conversely, for model-based methods like EAGLE, integrating SAM-Decoding tends to decrease the average number of accepted tokens and the generation throughput.

Turning to the contextual question answering dataset HAGRID, this task is highly conducive to retrieval methods, and SAM-Decoding effectively enhances inference speed. When SAM-Decoding is paired with Token Recycling, EAGLE, and EAGLE2, their inference speeds on the HAGRID dataset increase from  $1.93\times$ ,  $2.11\times$ , and  $2.41\times$  to  $2.57$ ,  $2.72$ , and  $2.81$ , respectively. It is also evident that the model-free method SAM-Decoding[T] achieves a higher speedup on this dataset compared to the state-of-the-art model-based method EAGLE2.

In addition to Vicuna-7B, we also conducted experiments on more models, and the experimental

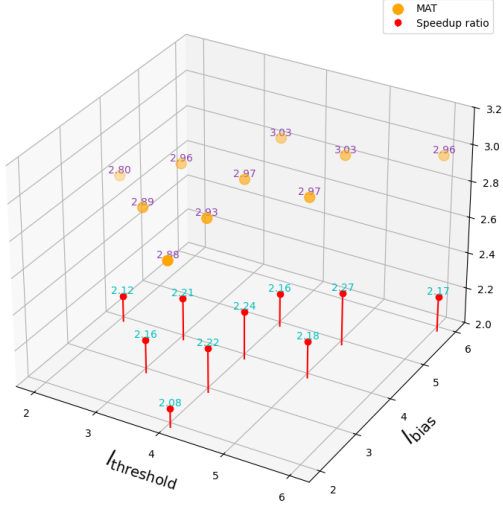


Figure 2: The speedup ratio and mean accepted tokens of SAM-Decoding[T] under different  $l_{bias}$  and  $l_{threshold}$ .

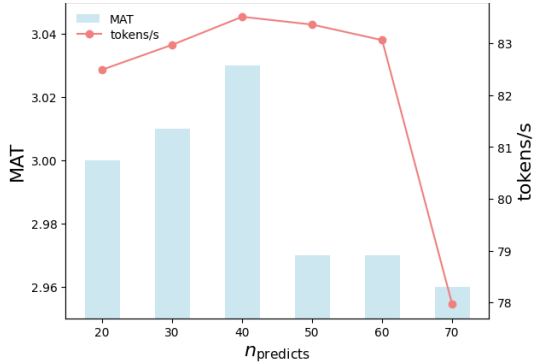


Figure 3: The speedup ratio and mean accepted tokens of SAM-Decoding[T] under different draft size.

results are shown in Appendix B.

**Ablation Experiments.** To further understand the contributions of various components of SAM-Decoding and the influence of different hyperparameters on inference speed, we conducted a series of ablation studies. Unless otherwise stated, these experiments were carried out on Spec-Bench using the vicuna-7B-v1.3 model, with SAM-Decoding[T] serving as the decoding strategy.

Firstly, we examined the effects of  $l_{bias}$  and  $l_{threshold}$  on inference speed through a grid search. These parameters control the preference for generating text from the generating text during retrieval and the preference for using retrieval results over the draft model when creating drafts. The findings are summarized in Figure 2. As shown, both the mean accepted tokens (MAT) and the speedup ratio increase with  $l_{bias}$  and  $l_{threshold}$  up to a point. Be-

Table 3: The impact of different draft generation modules on inference speed.

Method	Spec-Bench		
	#MAT	Tokens/s	Speedup
SAM-Decoding[T]	3.03	85.73	2.27 $\times$
w/o Static SAM	3.01	84.46	2.23 $\times$
w/o Dynamic SAM	2.68	76.14	2.01 $\times$
w/o Token Recycling	1.89	62.26	1.65 $\times$

yond a value of 5 for both parameters, these metrics start to decline.

Additionally, we investigated how the draft size utilized by SAM-Decoding affects inference speed. Figure 3 illustrates the mean accepted tokens and the inference speed of SAM-Decoding[T] at varying draft sizes. The data indicate that as the draft size grows, the mean number of accepted tokens and inference speed initially rise. However, once the draft size surpasses 40, these metrics begin to decline, and the decrease becomes more pronounced when the draft size reaches 70.

Finally, we investigated the impact of different modules within SAM-Decoding on inference speed. SAM-Decoding comprises three draft generation modules: the static suffix automaton, the dynamic suffix automaton, and the auxiliary speculative decoding module. We measured the inference speed of SAM-Decoding after removing each of these three modules individually. The results are presented in Table 3. From the experimental results, it is clear that each module contributes to the acceleration of the decoding process. Notably, the dynamic suffix automaton has a significantly greater impact compared to the static suffix automaton. This suggests that, in many cases, generating drafts from the dynamic context is more effective than retrieving drafts from a pre-existing text corpus. Additionally, since not all scenarios are well-suited for retrieval-based methods, the auxiliary speculative decoding module plays a crucial role in enhancing the overall performance of SAM-Decoding.

For more ablation experiment results, please refer to Appendix C.

## 5 Related Work

**Speculative Decoding.** Speculative decoding is an approach that can significantly speed up large language models (LLMs) without compromising the quality of their outputs. This is achieved by

increasing the number of tokens produced in each inference step while simultaneously decreasing the total number of inference steps required. The majority of speculative decoding techniques rely on smaller neural networks to create initial drafts during the inference process. These techniques are referred to as **model-based** speculative decoding methods. Early implementations of model-based speculative decoding, such as those described in Speculative Decoding (Leviathan et al., 2023), primarily focused on generating draft sequences using pre-existing, smaller-scale LLMs. Subsequently, advancements like Medusa (Cai et al., 2024) and SpecInfer (Miao et al., 2024) introduced tree-based speculative methods and initiated the development of dedicated draft models tailored for speculative decoding. For instance, Medusa developed a set of specialized decoding heads designed to serve as draft models. More recently, EAGLE (Li et al., 2024b,a) highlighted the significance of incorporating the hidden state of the model’s output into the speculative decoding process. In line with this insight, EAGLE trained a draft model that integrates the hidden state information from the model’s output, leading to more efficient acceleration across a range of tasks.

In contrast to model-based methods, certain approaches focus on generating drafts by leveraging the model’s recent prediction outcomes, such as the output from the decoding head. Examples of such methods include Lookahead Decoding (Fu et al., 2024) and Token Recycling (Luo et al., 2024). Lookahead Decoding keeps track of the  $n$ -grams of the generated text, whereas Token Recycling maintains the top  $k$  probable next tokens for each tokens.

Moreover, some strategies generate drafts directly through the retrieval of previously generated texts or text corpora, utilizing  $n$ -gram matching. Notable among these are PLD (Saxena, 2023) and REST (He et al., 2024). Our proposed SAM-Decoding method also employs retrieval for draft generation. However, it stands out due to its superior speed and accuracy, and it can be seamlessly integrated with other speculative decoding techniques.

Additionally, beyond the aforementioned methods, research also conducted on speculative decoding that relies either on the model itself (Kou et al., 2024) or on sub-models within the larger architecture (Elhoushi et al., 2024).

**Efficient LLM Architecture.** There is also work to improve the model’s inference speed from the perspective of model structure. This part of the work includes model distillation, quantization and pruning. Model distillation (Sreenivas et al., 2024; Muralidharan et al., 2024) distills the knowledge of a large model into a small model, thereby speeding up inference while maintaining the model’s performance. Quantization (Frantar et al., 2022; Xiao et al., 2023; Lin et al., 2024; Liu et al., 2024; Ashkboos et al., 2024b) reduces the number of bits required to store parameters and reduces the data transmission time from HBM to on-chip memory during inference, thereby achieving effective inference acceleration. Pruning (Frantar and Alistarh, 2023; Ashkboos et al., 2024a; Men et al., 2024; Chen et al., 2024; Hu et al., 2024; Sun et al., 2024; Zhang et al., 2024) is used to remove unimportant parameters in the model. For structured pruning, it can be combined with model distillation to train efficient small models, while semi-structured pruning can reduce the model’s memory access and computing overhead and improve the inference speed by combining special hardware, i.e., sparse tensor core.

## 6 Conclusion

In this work, we propose SAM-Decoding, an speculative decoding method via suffix automaton constructed from both generated text and text corpus. SAM-Decoding can efficiently retrieve drafts from retrieval sources, thereby accelerating inference. SAM-Decoding is also designed to seamlessly integrate with existing methods. Consequently, in scenarios where retrieval is not feasible, SAM-Decoding can adaptively switch to alternative methods for draft generation. Experimental results demonstrate that when combined with state-of-the-art techniques, SAM-Decoding can significantly enhance performance in multi-turn conversation, summarization, and retrieval-augmented generation tasks.

## References

Saleh Ashkboos, Maximilian L. Croci, Marcelo Gennari do Nascimento, Torsten Hoefer, and James Hensman. 2024a. *SliceGPT: Compress large language models by deleting rows and columns*. *Preprint*, arXiv:2401.15024.

Saleh Ashkboos, Amirkeivan Mohtashami, Maximilian L Croci, Bo Li, Pashmina Cameron, Martin Jaggi,

Dan Alistarh, Torsten Hoefer, and James Hensman. 2024b. Quarot: Outlier-free 4-bit inference in rotated llms. *arXiv preprint arXiv:2404.00456*.

Jacob Austin, Augustus Odena, Maxwell Nye, Maarten Bosma, Henryk Michalewski, David Dohan, Ellen Jiang, Carrie Cai, Michael Terry, Quoc Le, et al. 2021. Program synthesis with large language models. *arXiv preprint arXiv:2108.07732*.

Anselm Blumer, Janet Blumer, Andrzej Ehrenfeucht, David Haussler, and Ross McConnell. 1984. Building the minimal dfa for the set of all subwords of a word on-line in linear time. In *Automata, Languages and Programming: 11th Colloquium Antwerp, Belgium, July 16–20, 1984 11*, pages 109–118. Springer.

Tom B. Brown, Benjamin Mann, Nick Ryder, Melanie Subbiah, Jared Kaplan, Prafulla Dhariwal, Arvind Neelakantan, Pranav Shyam, Girish Sastry, Amanda Askell, Sandhini Agarwal, Ariel Herbert-Voss, Gretchen Krueger, Tom Henighan, Rewon Child, Aditya Ramesh, Daniel M. Ziegler, Jeffrey Wu, Clemens Winter, Christopher Hesse, Mark Chen, Eric Sigler, Mateusz Litwin, Scott Gray, Benjamin Chess, Jack Clark, Christopher Berner, Sam McCandlish, Alec Radford, Ilya Sutskever, and Dario Amodei. 2020. [Language models are few-shot learners](#). *Preprint*, arXiv:2005.14165.

Tianle Cai, Yuhong Li, Zhengyang Geng, Hongwu Peng, Jason D Lee, Deming Chen, and Tri Dao. 2024. Medusa: Simple llm inference acceleration framework with multiple decoding heads. *arXiv preprint arXiv:2401.10774*.

Mark Chen, Jerry Tworek, Heewoo Jun, Qiming Yuan, Henrique Ponde De Oliveira Pinto, Jared Kaplan, Harri Edwards, Yuri Burda, Nicholas Joseph, Greg Brockman, et al. 2021. Evaluating large language models trained on code. *arXiv preprint arXiv:2107.03374*.

Xiaodong Chen, Yuxuan Hu, Jing Zhang, Yanling Wang, Cuiping Li, and Hong Chen. 2024. [Streamlining redundant layers to compress large language models](#). *Preprint*, arXiv:2403.19135.

Karl Cobbe, Vineet Kosaraju, Mohammad Bavarian, Mark Chen, Heewoo Jun, Lukasz Kaiser, Matthias Plappert, Jerry Tworek, Jacob Hilton, Reiichiro Nakano, et al. 2021. Training verifiers to solve math word problems. *arXiv preprint arXiv:2110.14168*.

Abhimanyu Dubey, Abhinav Jauhri, Abhinav Pandey, Abhishek Kadian, Ahmad Al-Dahle, Aiesha Letman, Akhil Mathur, Alan Schelten, Amy Yang, Angela Fan, Anirudh Goyal, Anthony Hartshorn, Aobo Yang, Archi Mitra, Archie Sravankumar, Artem Korenev, Arthur Hinsvark, Arun Rao, Aston Zhang, Aurelien Rodriguez, Austen Gregerson, Ava Spataru, Baptiste Roziere, Bethany Biron, Bin Tang, Bobbie Chern, Charlotte Caucheteux, Chaya Nayak, Chloe Bi, Chris Marra, Chris McConnell, Christian Keller, Christophe Touret, Chunyang Wu, Corinne Wong, Cristian Canton Ferrer, Cyrus Nikolaidis, Damien Al-lonsius, Daniel Song, Danielle Pintz, Danny Livshits, David Esiobu, Dhruv Choudhary, Dhruv Mahajan, Diego Garcia-Olano, Diego Perino, Dieuwke Hupkes, Egor Lakomkin, Ehab AlBadawy, Elina Lobanova, Emily Dinan, Eric Michael Smith, Filip Radenovic, Frank Zhang, Gabriel Synnaeve, Gabrielle Lee, Georgia Lewis Anderson, Graeme Nail, Gregoire Milon, Guan Pang, Guillem Cucurell, Hailey Nguyen, Hannah Korevaar, Hu Xu, Hugo Touvron, Iliyan Zarov, Imanol Arrieta Ibarra, Isabel Kloumann, Ishan Misra, Ivan Evtimov, Jade Copet, Jaewon Lee, Jan Geffert, Jana Vranes, Jason Park, Jay Mahadeokar, Jeet Shah, Jelmer van der Linde, Jennifer Billock, Jenny Hong, Jenya Lee, Jeremy Fu, Jianfeng Chi, Jianyu Huang, Jiawen Liu, Jie Wang, Jiecao Yu, Joanna Bitton, Joe Spisak, Jongsoo Park, Joseph Rocca, Joshua Johnstun, Joshua Saxe, Junteng Jia, Kalyan Vasudevan Alwala, Kartikeya Upasani, Kate Plawiak, Ke Li, Kenneth Heafield, Kevin Stone, Khalid El-Arini, Krithika Iyer, Kshitiz Malik, Kuenley Chiu, Kunal Bhalla, Lauren Rantala-Yeary, Laurens van der Maaten, Lawrence Chen, Liang Tan, Liz Jenkins, Louis Martin, Lovish Madaan, Lubo Malo, Lukas Blecher, Lukas Landzaat, Luke de Oliveira, Madeline Muzzi, Mahesh Pasupuleti, Mannat Singh, Manohar Paluri, Marcin Kardas, Mathew Oldham, Mathieu Rita, Maya Pavlova, Melanie Kambadur, Mike Lewis, Min Si, Mitesh Kumar Singh, Mona Hassan, Naman Goyal, Narjes Torabi, Nikolay Bashlykov, Nikolay Bogoychev, Niladri Chatterji, Olivier Duchenne, Onur Çelebi, Patrick Alrassy, Pengchuan Zhang, Pengwei Li, Petar Vasic, Peter Weng, Prajwal Bhargava, Pratik Dubal, Praveen Krishnan, Punit Singh Koura, Puxin Xu, Qing He, Qingxiao Dong, Ragavan Srinivasan, Raj Ganapathy, Ramon Calderer, Ricardo Silveira Cabral, Robert Stojnic, Roberta Raileanu, Rohit Girdhar, Rohit Patel, Romain Sauvestre, Ronnie Polidoro, Roshan Sumbaly, Ross Taylor, Ruan Silva, Rui Hou, Rui Wang, Saghar Hosseini, Sahana Chennabasappa, Sanjay Singh, Sean Bell, Seohyun Sonia Kim, Sergey Edunov, Shaoliang Nie, Sharan Narang, Sharath Raparthy, Sheng Shen, Shengye Wan, Shruti Bhosale, Shun Zhang, Simon Vandenhende, Soumya Batra, Spencer Whitman, Sten Sootla, Stephane Collot, Suchin Gururangan, Sydney Borodinsky, Tamar Herman, Tara Fowler, Tarek Sheasha, Thomas Georgiou, Thomas Scialom, Tobias Speckbacher, Todor Mihaylov, Tong Xiao, Ujjwal Karn, Vedanuj Goswami, Vibhor Gupta, Vignesh Ramanathan, Viktor Kerkez, Vincent Gonguet, Virginie Do, Vish Vogeti, Vladan Petrovic, Weiwei Chu, Wenhan Xiong, Wenyin Fu, Whitney Meers, Xavier Martinet, Xiaodong Wang, Xiaoqing Ellen Tan, Xinfeng Xie, Xuchao Jia, Xuewei Wang, Yaelle Goldschlag, Yashesh Gaur, Yasmine Babaei, Yi Wen, Yiwen Song, Yuchen Zhang, Yue Li, Yuning Mao, Zacharie Delpierre Coudert, Zheng Yan, Zhengxing Chen, Zoe Papakipos, Aaditya Singh, Aaron Grattafiori, Abha Jain, Adam Kelsey, Adam Shajnfeld, Adithya Gangidi, Adolfo Victoria, Ahuva Goldstand, Ajay Menon, Ajay Sharma, Alex Boesenberg, Alex Vaughan, Alexei Baevski, Allie Feinstein, Amanda Kallet, Amit Sangani, Anam Yunus, An-

drei Lupu, Andres Alvarado, Andrew Caples, Andrew Gu, Andrew Ho, Andrew Poulton, Andrew Ryan, Ankit Ramchandani, Annie Franco, Aparajita Saraf, Arkabandhu Chowdhury, Ashley Gabriel, Ashwin Bharambe, Assaf Eisenman, Azadeh Yazdan, Beau James, Ben Maurer, Benjamin Leonhardi, Bernie Huang, Beth Loyd, Beto De Paola, Bhargavi Paranjape, Bing Liu, Bo Wu, Boyu Ni, Braden Hancock, Bram Wasti, Brandon Spence, Brani Stojkovic, Brian Gamido, Britt Montalvo, Carl Parker, Carly Burton, Catalina Mejia, Changhan Wang, Changkyu Kim, Chao Zhou, Chester Hu, Ching-Hsiang Chu, Chris Cai, Chris Tindal, Christoph Feichtenhofer, Damon Civin, Dana Beaty, Daniel Kreymer, Daniel Li, Danny Wyatt, David Adkins, David Xu, Davide Testuggine, Delia David, Devi Parikh, Diana Liskovich, Didem Foss, Dingkang Wang, Duc Le, Dustin Holland, Edward Dowling, Eissa Jamil, Elaine Montgomery, Eleonora Presani, Emily Hahn, Emily Wood, Erik Brinkman, Esteban Arcaute, Evan Dunbar, Evan Smothers, Fei Sun, Felix Kreuk, Feng Tian, Firat Ozgenel, Francesco Caggioni, Francisco Guzmán, Frank Kanayet, Frank Seide, Gabriela Medina Florez, Gabriella Schwarz, Gada Badeer, Georgia Swee, Gil Halpern, Govind Thattai, Grant Herman, Grigory Sizov, Guangyi, Zhang, Guna Lakshminarayanan, Hamid Shojanazeri, Han Zou, Hannah Wang, Hanwen Zha, Haroun Habeeb, Harrison Rudolph, Helen Suk, Henry Asperegn, Hunter Goldman, Ibrahim Damlaj, Igor Molybog, Igor Tufanov, Irina-Elena Veliche, Itai Gat, Jake Weissman, James Geboski, James Kohli, Japhet Asher, Jean-Baptiste Gaya, Jeff Marcus, Jeff Tang, Jennifer Chan, Jenny Zhen, Jeremy Reizenstein, Jeremy Teboul, Jessica Zhong, Jian Jin, Jingyi Yang, Joe Cummings, Jon Carvill, Jon Shepard, Jonathan McPhie, Jonathan Torres, Josh Ginsburg, Junjie Wang, Kai Wu, Kam Hou U, Karan Saxena, Karthik Prasad, Kartikay Khandelwal, Katayoun Zand, Kathy Matosich, Kaushik Veeraraghavan, Kelly Michelena, Keqian Li, Kun Huang, Kunal Chawla, Kushal Lakhotia, Kyle Huang, Lailin Chen, Lakshya Garg, Lavender A, Leandro Silva, Lee Bell, Lei Zhang, Liangpeng Guo, Licheng Yu, Liron Moshkovich, Luca Wehrstedt, Madien Khabsa, Manav Avalani, Manish Bhatt, Maria Tsimpoukelli, Martynas Mankus, Matan Hasson, Matthew Lennie, Matthias Reso, Maxim Groshev, Maxim Naumov, Maya Lathi, Meghan Keneally, Michael L. Seltzer, Michal Valko, Michelle Restrepo, Mihir Patel, Mik Vyatskov, Mikayel Samvelyan, Mike Clark, Mike Macey, Mike Wang, Miquel Jubert Hermoso, Mo Metanat, Mohammad Rastegari, Munish Bansal, Nandhini Santhanam, Natascha Parks, Natasha White, Navyata Bawa, Nayan Singhal, Nick Egebo, Nicolas Usunier, Nikolay Pavlovich Laptev, Ning Dong, Ning Zhang, Norman Cheng, Oleg Chernoguz, Olivia Hart, Omkar Salpekar, Ozlem Kalinli, Parkin Kent, Parth Parekh, Paul Saab, Parvan Balaji, Pedro Rittner, Philip Bontrager, Pierre Roux, Piotr Dollar, Polina Zvyagina, Prashant Ratanchandani, Pritish Yuvraj, Qian Liang, Rachad Alao, Rachel Rodriguez, Rafi Ayub, Raghatham Murthy, Raghu Nayani, Rahul Mitra, Raymond Li, Rebekkah Hogan, Robin Battey, Rocky Wang, Rohan Maheswari, Russ Howes, Ruty Rinott, Sai Jayesh Bondu, Samyak Datta, Sara Chugh, Sara Hunt, Sargun Dhillon, Sasha Sidorov, Satadru Pan, Saurabh Verma, Seiji Yamamoto, Sharadh Ramaswamy, Shaun Lindsay, Shaun Lindsay, Sheng Feng, Shenghao Lin, Shengxin Cindy Zha, Shiva Shankar, Shuqiang Zhang, Shuqiang Zhang, Sinong Wang, Sneha Agarwal, Soji Sajuyigbe, Soumith Chintala, Stephanie Max, Stephen Chen, Steve Kehoe, Steve Satterfield, Sudarshan Govindaprasad, Sumit Gupta, Sungmin Cho, Sunny Virk, Suraj Subramanian, Sy Choudhury, Sydney Goldman, Tal Remez, Tamar Glaser, Tamara Best, Thilo Kohler, Thomas Robinson, Tianhe Li, Tianjun Zhang, Tim Matthews, Timothy Chou, Tzook Shaked, Varun Vontimitta, Victoria Ajayi, Victoria Montanez, Vijai Mohan, Vinay Satish Kumar, Vishal Mangla, Vitor Albiero, Vlad Ionescu, Vlad Poenaru, Vlad Tiberiu Mihailescu, Vladimir Ivanov, Wei Li, Wencheng Wang, Wenwen Jiang, Wes Bouaziz, Will Constable, Xiaocheng Tang, Xiaofang Wang, Xiaojian Wu, Xiaolan Wang, Xide Xia, Xilun Wu, Xinbo Gao, Yanjun Chen, Ye Hu, Ye Jia, Ye Qi, Yenda Li, Yilin Zhang, Ying Zhang, Yossi Adi, Youngjin Nam, Yu, Wang, Yuchen Hao, Yundi Qian, Yuzi He, Zach Rait, Zachary DeVito, Zef Rosnbrick, Zhaoduo Wen, Zhenyu Yang, and Zhiwei Zhao. 2024. *The llama 3 herd of models*. *Preprint*, arXiv:2407.21783.

Mostafa Elhoushi, Akshat Shrivastava, Diana Liskovich, Basil Hosmer, Bram Wasti, Liangzhen Lai, Anas Mahmoud, Bilge Acun, Saurabh Agarwal, Ahmed Roman, et al. 2024. Layer skip: Enabling early exit inference and self-speculative decoding. *arXiv preprint arXiv:2404.16710*.

Elias Frantar and Dan Alistarh. 2023. *Sparsegpt: Massive language models can be accurately pruned in one-shot*. *Preprint*, arXiv:2301.00774.

Elias Frantar, Saleh Ashkboos, Torsten Hoefer, and Dan Alistarh. 2022. Gptq: Accurate post-training quantization for generative pre-trained transformers. *arXiv preprint arXiv:2210.17323*.

Yichao Fu, Peter Bailis, Ion Stoica, and Hao Zhang. 2024. Break the sequential dependency of llm inference using lookahead decoding. *arXiv preprint arXiv:2402.02057*.

Zhenyu He, Zexuan Zhong, Tianle Cai, Jason Lee, and Di He. 2024. Rest: Retrieval-based speculative decoding. In *Proceedings of the 2024 Conference of the North American Chapter of the Association for Computational Linguistics: Human Language Technologies (Volume 1: Long Papers)*, pages 1582–1595.

Yuxuan Hu, Jing Zhang, Zhe Zhao, Chen Zhao, Xiaodong Chen, Cuiping Li, and Hong Chen. 2024. Sp<sup>3</sup>: Enhancing structured pruning via pca projection. *Preprint*, arXiv:2308.16475.

Ehsan Kamalloo, Aref Jafari, Xinyu Zhang, Nandan Thakur, and Jimmy Lin. 2023. Hagrid: A human-llm collaborative dataset for generative information-seeking with attribution. *arXiv preprint arXiv:2307.16883*.

Vladimir Karpukhin, Barlas Oğuz, Sewon Min, Patrick Lewis, Ledell Wu, Sergey Edunov, Danqi Chen, and Wen-tau Yih. 2020. Dense passage retrieval for open-domain question answering. *arXiv preprint arXiv:2004.04906*.

Siqi Kou, Lanxiang Hu, Zhezhi He, Zhijie Deng, and Hao Zhang. 2024. Cllms: Consistency large language models. *arXiv preprint arXiv:2403.00835*.

Tom Kwiatkowski, Jennimaria Palomaki, Olivia Redfield, Michael Collins, Ankur Parikh, Chris Alberti, Danielle Epstein, Illia Polosukhin, Jacob Devlin, Kenton Lee, Kristina Toutanova, Llion Jones, Matthew Kelcey, Ming-Wei Chang, Andrew M. Dai, Jakob Uszkoreit, Quoc Le, and Slav Petrov. 2019. **Natural questions: A benchmark for question answering research**. *Transactions of the Association for Computational Linguistics*, 7:452–466.

Yaniv Leviathan, Matan Kalman, and Yossi Matias. 2023. Fast inference from transformers via speculative decoding. In *International Conference on Machine Learning*, pages 19274–19286. PMLR.

Yuhui Li, Fangyun Wei, Chao Zhang, and Hongyang Zhang. 2024a. Eagle-2: Faster inference of language models with dynamic draft trees. *arXiv preprint arXiv:2406.16858*.

Yuhui Li, Fangyun Wei, Chao Zhang, and Hongyang Zhang. 2024b. Eagle: Speculative sampling requires rethinking feature uncertainty. *arXiv preprint arXiv:2401.15077*.

Ji Lin, Jiaming Tang, Haotian Tang, Shang Yang, Wei-Ming Chen, Wei-Chen Wang, Guangxuan Xiao, Xingyu Dang, Chuang Gan, and Song Han. 2024. Awq: Activation-aware weight quantization for on-device llm compression and acceleration. *Proceedings of Machine Learning and Systems*, 6:87–100.

Zechun Liu, Changsheng Zhao, Igor Fedorov, Bilge Soran, Dhruv Choudhary, Raghuraman Krishnamoorthi, Vikas Chandra, Yuandong Tian, and Tijmen Blankevoort. 2024. Spinquant–llm quantization with learned rotations. *arXiv preprint arXiv:2405.16406*.

Xianzhen Luo, Yixuan Wang, Qingfu Zhu, Zhiming Zhang, Xuanyu Zhang, Qing Yang, Dongliang Xu, and Wanxiang Che. 2024. Turning trash into treasure: Accelerating inference of large language models with token recycling. *arXiv preprint arXiv:2408.08696*.

Xin Men, Mingyu Xu, Qingyu Zhang, Bingning Wang, Hongyu Lin, Yaojie Lu, Xianpei Han, and Weipeng Chen. 2024. **Shortgpt: Layers in large language models are more redundant than you expect**. Preprint, arXiv:2403.03853.

Xupeng Miao, Gabriele Oliaro, Zhihao Zhang, Xinhao Cheng, Zeyu Wang, Zhengxin Zhang, Rae Ying Yee Wong, Alan Zhu, Lijie Yang, Xiaoxiang Shi, et al. 2024. Specinfer: Accelerating large language model serving with tree-based speculative inference and verification. In *Proceedings of the 29th ACM International Conference on Architectural Support for Programming Languages and Operating Systems, Volume 3*, pages 932–949.

Saurav Muralidharan, Sharath Turuvekere Sreenivas, Raviraj Joshi, Marcin Chochowski, Mostafa Patwary, Mohammad Shoeybi, Bryan Catanzaro, Jan Kautz, and Pavlo Molchanov. 2024. **Compact language models via pruning and knowledge distillation**. Preprint, arXiv:2407.14679.

Ramesh Nallapati, Bowen Zhou, Caglar Gulcehre, Bing Xiang, et al. 2016. Abstractive text summarization using sequence-to-sequence rnns and beyond. *arXiv preprint arXiv:1602.06023*.

Apoorv Saxena. 2023. **Prompt lookup decoding**.

Sharath Turuvekere Sreenivas, Saurav Muralidharan, Raviraj Joshi, Marcin Chochowski, Mostafa Patwary, Mohammad Shoeybi, Bryan Catanzaro, Jan Kautz, and Pavlo Molchanov. 2024. Llm pruning and distillation in practice: The minitron approach. *arXiv preprint arXiv:2408.11796*.

Mingjie Sun, Zhuang Liu, Anna Bair, and J. Zico Kolter. 2024. **A simple and effective pruning approach for large language models**. Preprint, arXiv:2306.11695.

Heming Xia, Zhe Yang, Qingxiu Dong, Peiyi Wang, Yongqi Li, Tao Ge, Tianyu Liu, Wenjie Li, and Zhifang Sui. 2024. Unlocking efficiency in large language model inference: A comprehensive survey of speculative decoding. *arXiv preprint arXiv:2401.07851*.

Guangxuan Xiao, Ji Lin, Mickael Seznec, Hao Wu, Julien Demouth, and Song Han. 2023. Smoothquant: Accurate and efficient post-training quantization for large language models. In *International Conference on Machine Learning*, pages 38087–38099. PMLR.

An Yang, Baosong Yang, Binyuan Hui, Bo Zheng, Bowen Yu, Chang Zhou, Chengpeng Li, Chengyuan Li, Dayiheng Liu, Fei Huang, et al. 2024. Qwen2 technical report. *arXiv preprint arXiv:2407.10671*.

Yingtao Zhang, Haoli Bai, Haokun Lin, Jialin Zhao, Lu Hou, and Carlo Vittorio Cannistraci. 2024. **Plug-and-play: An efficient post-training pruning method for large language models**. In *The Twelfth International Conference on Learning Representations*.

Lianmin Zheng, Wei-Lin Chiang, Ying Sheng, Siyuan Zhuang, Zhanghao Wu, Yonghao Zhuang, Zi Lin, Zhuohan Li, Dacheng Li, Eric Xing, et al. 2023. Judging llm-as-a-judge with mt-bench and chatbot arena. *Advances in Neural Information Processing Systems*, 36:46595–46623.

## A Suffix Automaton

### A.1 Construction Process of Suffix Automaton

Algorithm 3 introduces the construction (Build-SAM) and expansion process (Expand) of Suffix

Automaton, where INIT\_SAM function will create a suffix automaton that only contains the root node. And for the root node, the **link** attribute value is  $-1$ , the **next** attribute value is empty, the length attribute value is  $0$ , and the min\_endpos attribute value is  $0$ .

## A.2 Time Complexity of State Transfer

In this section, we introduce the time complexity of state transfer of suffix automaton. Consider a suffix automaton  $S$  with initial state  $s_0$ , which corresponds to the root node of the automaton (representing the empty string). Suppose that state  $s_0$  undergoes transitions through a sequence of  $L$  tokens  $x = (x_1, x_2, \dots, x_L)$ :

$$s_i = \text{Transfer}(S, x_i, s_{i-1}), \quad i \in \{1, 2, \dots, L\}.$$

We aim to demonstrate that the average time complexity of each state transition is  $O(1)$ , while the worst-case time complexity is  $O(L)$ .

First, let us define the matching length associated with state  $s_i$  as  $l_i$ . Given that each state transition can increase the length of the match by at most 1, it follows that  $0 \leq l_i \leq i$ . Next, we introduce the concept of energy  $\phi$  for each state  $s_i$ , defined as  $\phi(s_i) = l_i$ . Let  $c_i$  represent the time cost of the transition of the  $i$ -th state. We then define the amortized cost  $\hat{c}_i$  as:

$$\hat{c}_i = c_i + \phi(s_i) - \phi(s_{i-1}).$$

We can now express the total amortized cost over all transitions as:

$$\begin{aligned} \sum_{i=1}^L \hat{c}_i &= \sum_{i=1}^L (c_i + \phi(s_i) - \phi(s_{i-1})) \\ &= \sum_{i=1}^L c_i + \phi(s_L) - \phi(s_0). \end{aligned}$$

Since  $\phi(s_i) \geq 0$  and  $\phi(s_0) = 0$ , it follows that:

$$\sum_{i=1}^L \hat{c}_i \geq \sum_{i=1}^L c_i.$$

Next, we analyze the upper bound of  $\hat{c}_i$ . Each state transition involves moving through the **link** edge zero or more times, followed by a move through the **next** edge. Transitioning through the **link** edge incurs a cost of 1 but decreases the potential by at least 1. Conversely, transitioning through

the **next** edge also incurs a cost of 1 but increases the potential by 1. Consequently, the amortized cost  $\hat{c}_i$  is bounded above by 2, leading to:

$$\sum_{i=1}^L \hat{c}_i \leq 2L.$$

Thus, the average time complexity of state transitions is:

$$\frac{\sum_{i=1}^L \hat{c}_i}{L} \leq \frac{2L}{L} = 2,$$

which is  $O(1)$ . In the worst case, a single operation may require up to  $l_i$  transitions through the **link** edge, followed by one transition through the **next** edge, resulting in a worst-case time complexity of  $O(L)$ .

## B Additional Experiment Results

In this section, we present the results of the experiment on Llama3-8B-instruct.

Tables 4 and 5 present the speedup ratios of SAM-Decoding compared to baseline methods across the Spec-Bench, HumanEval, MBPP, and HAGRID datasets, utilizing the Llama3-8B-instruct model. In particular, SAM-Decoding, when paired with Token Recycling (SAM-Decoding[T]), brings speedups on all tasks and achieves the highest average speedup. Specifically, SAM-Decoding enhances the speedup ratio of Token Recycling from  $1.92\times$ ,  $1.85\times$ , and  $1.82\times$  to  $2.09\times$ ,  $2.04\times$ , and  $2.12\times$  for multi-turn conversation, summarization, and retrieval-augmented generation tasks, respectively. This improvement raises the overall speedup ratio of token recycling in the Spec-Bench dataset from  $1.91\times$  to  $2.05\times$ . On the HumanEval and MBPP datasets, SAM-Decoding increases the speedup ratio of Token Recycling from  $1.80\times$  and  $2.04\times$  to  $2.27\times$  and  $2.37\times$ , respectively. For the HAGRID dataset, the integration of SAM-Decoding with Token Recycling increases the speedup ratio from  $1.87\times$  to  $1.99\times$ . Furthermore, beyond enhancing Token Recycling, SAM-Decoding also amplifies the performance gains of EAGLE2 in multi-turn conversation, summarization, retrieval-augmented generation, and context Q&A tasks. The speedup ratios were increased from  $2.08\times$ ,  $1.85\times$ ,  $1.87\times$ , and  $1.86\times$  to  $2.23\times$ ,  $1.93\times$ ,  $2.06\times$ , and  $2.02\times$  respectively.

Model	Method	Multi-turn Conversation	Translation	Summarization	Question Answering	Mathematical Reasoning	Retrieval-aug. Generation	#Mean Accepted Tokens	Tokens/s	Overall
Llama3-8B-Inst	PLD	1.30×	1.12×	1.41×	1.03×	1.30×	1.53×	1.39	44.26	1.28×
	Token Recycling	1.92×	1.88×	1.85×	1.75×	2.24×	1.82×	2.76	66.42	1.91×
	<b>SAM-Decoding[T]</b>	2.09×	1.93×	2.04×	1.82×	2.32×	2.12×	2.63	85.73	2.05×
	EAGLE2	2.08×	1.95×	1.85×	1.80×	2.31×	1.87×	3.90	68.69	1.98×
	<b>SAM-Decoding[E2]</b>	2.23×	1.92×	1.93×	1.76×	2.23×	2.06×	3.91	70.40	2.03×

Table 4: Speedup of SAM-Decoding compared to the baselines on Spec-Bench.

Model	Method	HumanEval			MBPP			HAGRID		
		#MAT	Tokens/s	Speedup	#MAT	Tokens/s	Speedup	#MAT	Tokens/s	Speedup
Llama3-8B-Inst	PLD	1.30	42.39	1.18×	1.23	39.19	1.06×	1.50	45.15	1.34×
	Token Recycling	2.93	71.49	1.99×	2.89	74.05	2.02×	2.84	62.77	1.87×
	<b>SAM-Decoding[T]</b>	2.77	78.04	2.16×	2.65	76.76	2.09×	2.70	66.76	1.99×
	EAGLE2	4.74	85.58	2.37×	4.77	95.02	2.58×	3.97	63.30	1.86×
	<b>SAM-Decoding[E2]</b>	4.76	91.50	2.54×	4.34	89.15	2.43×	3.93	67.94	2.02×

Table 5: Speedup of SAM-Decoding compared to the baselines on HumanEval, MBPP, and HAGRID.

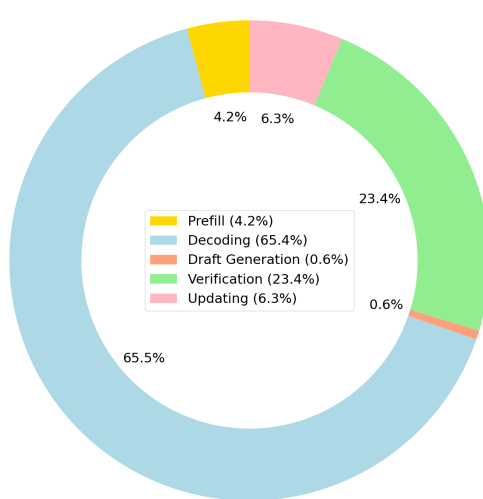


Figure 4: the percentage of inference time of different modules in SAM-Decoding.

### C Additional Ablation Experiments

In this section, we present additional ablation experiments, including the percentage of inference time of different modules in the decoding process of SAM-Decoding, and the percentage of drafts provided by different draft modules in SAM-Decoding.

The inference process of SAM-Decoding is divided into five stages: prefill, draft generation, decoding, verification, and updating. During the prefill stage, the model processes the input prompt to establish an initial state. In the draft generation stage, a draft is produced based on this initial state. The decoding stage involves the model fur-

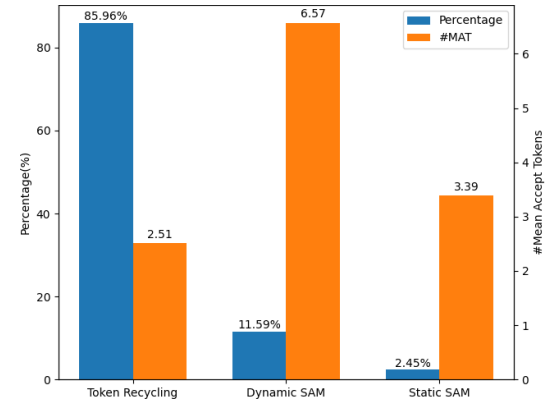


Figure 5: the percentage of usage times and mean accept tokens of different draft modules.

ther processing this draft. Next comes verification, where the correct parts of the draft are evaluated based on the information processed during the decoding stage. Finally, the update phase modifies the state of the model based on the valid parts of the draft. Figure 4 illustrates the proportion of time each stage consumes within the SAM-Decoding[T] process base on Spec-Bench. As shown, the decoding stage takes up the largest portion of time, accounting for 65.4% of the entire process. This is followed by the verification stage, which occupies 23.4% of the total time. The updating stage requires 6.3% of the time, whereas the draft generation stage contributes only 0.6% to the overall duration. Additionally, the prefill stage comprises 4.2% of the total processing time.

Figure 5 shows the usage times of different draft modules of SAM-Decoding[T] on Spec-Bench and

Model	Method	Multi-turn Conversation	Translation	Summarization	Question Answering	Mathematical Reasoning	Retrieval-aug. Generation	#Mean Accepted Tokens	Tokens/s	Overall
Vicuna-13B	PLD	1.61 $\times$	1.10 $\times$	2.36 $\times$	1.11 $\times$	1.69 $\times$	1.80 $\times$	1.66	33.89	1.59 $\times$
	Token Recycling	2.03 $\times$	1.84 $\times$	2.07 $\times$	1.83 $\times$	2.42 $\times$	1.84 $\times$	2.81	42.74	2.01 $\times$
	<b>SAM-Decoding[T]</b>	2.36 $\times$	1.80 $\times$	2.63 $\times$	1.83 $\times$	2.49 $\times$	2.22 $\times$	2.91	47.27	2.22 $\times$
	EAGLE2	3.10 $\times$	2.15 $\times$	2.58 $\times$	2.38 $\times$	3.19 $\times$	2.33 $\times$	4.42	56.06	2.63 $\times$
	<b>SAM-Decoding[E2]</b>	3.27 $\times$	2.12 $\times$	2.89 $\times$	2.34 $\times$	3.12 $\times$	2.54 $\times$	4.51	57.88	2.72 $\times$

Table 6: Speedup of SAM-Decoding compared to the baselines on Spec-Bench.

Model	Method	HumanEval			MBPP			HAGRID		
		#MAT	Tokens/s	Speedup	#MAT	Tokens/s	Speedup	#MAT	Tokens/s	Speedup
Vicuna-13B	PLD	1.54	32.06	1.44 $\times$	1.40	29.43	1.30 $\times$	1.90	43.38	2.15 $\times$
	Token Recycling	2.79	46.03	2.07 $\times$	2.85	48.89	2.16 $\times$	2.90	40.97	2.03 $\times$
	<b>SAM-Decoding[T]</b>	2.79	50.87	2.28 $\times$	2.83	52.14	2.30 $\times$	2.99	48.33	2.40 $\times$
	EAGLE2	5.15	77.85	3.49 $\times$	5.26	82.13	3.63 $\times$	4.24	52.28	2.59 $\times$
	<b>SAM-Decoding[E2]</b>	4.97	73.78	3.31 $\times$	4.80	73.94	3.27 $\times$	4.41	56.17	2.78 $\times$

Table 7: Speedup of SAM-Decoding compared to the baselines on HumanEval, MBPP, and HAGRID.

the corresponding average draft accept length. It can be seen that in 85.96% of the cases, due to insufficient matching length, we generate drafts based on the auxiliary method, corresponding to an average accept length of 2.51, while in the remaining 11.59% and 2.45% of the cases, the dynamic suffix automaton and static suffix automaton are used to generate drafts, corresponding to average accept lengths of 6.57 and 3.39, respectively.

Model	Method	Multi-turn Conversation	Translation	Summarization	Question Answering	Mathematical Reasoning	Retrieval-aug. Generation	#Mean Accepted Tokens	Tokens/s	Overall
Vicuna-33B	PLD	1.50 $\times$	1.07 $\times$	2.06 $\times$	1.09 $\times$	1.59 $\times$	1.51 $\times$	1.65	13.33	1.46 $\times$
	Token Recycling	2.10 $\times$	1.84 $\times$	2.19 $\times$	1.88 $\times$	2.42 $\times$	1.92 $\times$	2.70	18.8	2.06 $\times$
	<b>SAM-Decoding[T]</b>	2.31 $\times$	1.79 $\times$	2.53 $\times$	1.90 $\times$	2.48 $\times$	2.06 $\times$	2.68	19.87	2.18 $\times$
	EAGLE2	3.29 $\times$	2.31 $\times$	2.73 $\times$	2.51 $\times$	3.65 $\times$	2.46 $\times$	4.06	25.86	2.83 $\times$
	<b>SAM-Decoding[E2]</b>	3.36 $\times$	2.24 $\times$	2.88 $\times$	2.41 $\times$	3.43 $\times$	2.50 $\times$	4.08	25.60	2.81 $\times$

Table 8: Speedup of SAM-Decoding compared to the baselines on Spec-Bench.

Model	Method	HumanEval			MBPP			HAGRID		
		#MAT	Tokens/s	Speedup	#MAT	Tokens/s	Speedup	#MAT	Tokens/s	Speedup
Vicuna-33B	PLD	1.58	14.18	1.51 $\times$	1.34	11.82	1.30 $\times$	-	-	-
	Token Recycling	2.64	19.64	2.09 $\times$	2.76	20.92	2.19 $\times$	-	-	-
	<b>SAM-Decoding[T]</b>	2.73	22.44	2.39 $\times$	2.65	21.80	2.28 $\times$	2.60	19.74	2.26 $\times$
	EAGLE2	3.53	28.18	3.00 $\times$	5.04	37.35	3.91 $\times$	3.84	24.28	2.78 $\times$
	<b>SAM-Decoding[E2]</b>	3.61	29.49	3.14 $\times$	4.70	34.21	3.58 $\times$	3.79	24.45	2.80 $\times$

Table 9: Speedup of SAM-Decoding compared to the baselines on HumanEval, MBPP, and HAGRID.

Model	Method	Multi-turn Conversation	Translation	Summarization	Question Answering	Mathematical Reasoning	Retrieval-aug. Generation	#Mean Accepted Tokens	Tokens/s	Overall
Vicuna-7B	PLD	1.61 $\times$	1.56 $\times$	0.99 $\times$	2.47 $\times$	1.11 $\times$	1.51 $\times$	1.75	78.26	1.56 $\times$
	Token Recycling	2.08 $\times$	1.76 $\times$	1.97 $\times$	1.85 $\times$	2.35 $\times$	1.76 $\times$	2.82	98.39	1.96 $\times$
	<b>SAM-Decoding[T]</b>	2.62 $\times$	1.82 $\times$	2.92 $\times$	2.09 $\times$	2.60 $\times$	2.21 $\times$	3.02	119.21	2.38 $\times$
	EAGLE2	2.66 $\times$	1.76 $\times$	2.18 $\times$	2.03 $\times$	2.63 $\times$	1.97 $\times$	4.34	110.56	2.21 $\times$
	<b>SAM-Decoding[E2]</b>	3.19 $\times$	1.97 $\times$	2.86 $\times$	2.28 $\times$	2.84 $\times$	2.32 $\times$	4.52	129.36	2.58 $\times$

Table 10: Speedup of SAM-Decoding on A100 GPU compared to the baselines on Spec-Bench.

---

**Algorithm 3** Construction Process of Suffix Automaton

---

```
function Expand-State
  Input: suffix automaton  $S$ , link  $l$ , next  $n$ ,
  length  $len$ , position  $p$ 
   $s = S.\text{expand\_state}()$ 
   $s.\text{link} = l$ 
   $s.\text{next} = n$ 
   $s.\text{length} = len$ 
   $s.\text{min\_endpos} = p$ 
  return  $s$ 
end function
function Expand
  Input: suffix automaton  $S$ , token  $t$ 
   $S.\text{max\_length} = S.\text{max\_length} + 1$ 
   $l = S.\text{max\_length}$ 
   $c = \text{Expand-State}(S, -1, \{\}, l, l)$ 
   $p = S.\text{last}$ 
  while  $p \neq -1$  and  $t \notin p.\text{next}$  do
     $p.\text{next}[t] = c$ 
     $p = p.\text{link}$ 
  end while
  if  $p = \text{None}$  then
     $c.\text{link} = S.\text{root}$ 
  else
     $q = p.\text{next}[t]$ 
    if  $p.\text{length} + 1 = q.\text{length}$  then
       $c.\text{link} = q$ 
    else
       $cl = \text{Expand-State}(S, , -1, \{\}, -1, -1)$ 
       $cl.\text{link} = q.\text{link}$ 
       $cl.\text{next} = q.\text{next}$ 
       $cl.\text{length} = p.\text{length} + 1$ 
       $cl.\text{min\_endpos} = q.\text{min\_endpos}$ 
      while  $p \neq \text{None}$  and  $p.\text{next}[t] = q$  do
         $p.\text{next}[t] = cl$ 
         $p = p.\text{link}$ 
      end while
       $q.\text{link} = c.\text{link} = cl$ 
    end if
  end if
   $S.\text{last} = c$ 
end function
function Build-SAM
  Input: token sequence  $s$ 
   $S = \text{INIT\_SAM}()$ 
  for  $t$  in  $s$  do
     $\text{Expand}(S, t)$ 
  end for
  return  $S$ 
end function
```

---